Lecture Notes in Mechanical Engineering

Faiz Ahmad
Hussain H. Al-Kayiem
William Pao King Soon *Editors*

ICPER 2020

Proceedings of the 7th International Conference on Production, Energy and Reliability

Springer

Lecture Notes in Mechanical Engineering

Lecture Notes in Mechanical Engineering (LNME) publishes the latest developments in Mechanical Engineering—quickly, informally and with high quality. Original research reported in proceedings and post-proceedings represents the core of LNME. Volumes published in LNME embrace all aspects, subfields and new challenges of mechanical engineering. Topics in the series include:

- Engineering Design
- Machinery and Machine Elements
- Mechanical Structures and Stress Analysis
- Automotive Engineering
- Engine Technology
- Aerospace Technology and Astronautics
- Nanotechnology and Microengineering
- Control, Robotics, Mechatronics
- MEMS
- Theoretical and Applied Mechanics
- Dynamical Systems, Control
- Fluid Mechanics
- Engineering Thermodynamics, Heat and Mass Transfer
- Manufacturing
- Precision Engineering, Instrumentation, Measurement
- Materials Engineering
- Tribology and Surface Technology

To submit a proposal or request further information, please contact the Springer Editor of your location:

China: Ms. Ella Zhang at ella.zhang@springer.com
India: Priya Vyas at priya.vyas@springer.com
Rest of Asia, Australia, New Zealand: Swati Meherishi at swati.meherishi@springer.com
All other countries: Dr. Leontina Di Cecco at Leontina.dicecco@springer.com

To submit a proposal for a monograph, please check our Springer Tracts in Mechanical Engineering at https://link.springer.com/bookseries/11693 or contact Leontina.dicecco@springer.com

Indexed by SCOPUS. All books published in the series are submitted for consideration in Web of Science.

Faiz Ahmad · Hussain H. Al-Kayiem ·
William Pao King Soon
Editors

ICPER 2020

Proceedings of the 7th International Conference on Production, Energy and Reliability

Springer

Editors
Faiz Ahmad
Universiti Teknologi Petronas
Ipoh, Malaysia

Hussain H. Al-Kayiem
Universiti Teknologi Petronas
Ipoh, Malaysia

William Pao King Soon
Universiti Teknologi Petronas
Ipoh, Malaysia

ISSN 2195-4356 ISSN 2195-4364 (electronic)
Lecture Notes in Mechanical Engineering
ISBN 978-981-19-1938-1 ISBN 978-981-19-1939-8 (eBook)
https://doi.org/10.1007/978-981-19-1939-8

This Springer imprint is published by the registered company Springer Nature Singapore Pte Ltd.
The registered company address is: 152 Beach Road, #21-01/04 Gateway East, Singapore 189721, Singapore

Contents

Thermo-Fluids

Turbulent Flow Estimation by Wavelet Transform

A. B. Osman, Mark Ovinis, Ahmed Muftah Montaser Mihoob, Abdalellah O. Mohmmed, and Shafriza Nisha Basah

Abstract Turbulent flow estimation from an image sequence is challenging due to the lack of dedicated flow measurement techniques. Existing techniques estimate flowrate with high uncertainty. In this paper, a new technique based on discrete wavelet transform (DWT) is proposed. Wavelets have the advantage of decomposing flow signals into numerous levels and remove input signal noise. The flow signals are first decomposed using DWT into multiple levels, then, the wavelet coefficients are correlated by the Fast Fourier Transform (FFT) based algorithm to determine the velocity field. This wavelet-based algorithm is named as DWT-FFT. DWT-FFT was evaluated first using synthetic signals and then applied for turbulent flow estimation. The accuracy of DWT-FFT was compared to classical algorithms including direct cross correlation (DCC) and direct implementation of FFT. DWT-FFT estimated the flow with an error of 0.7%, outperforming both DCC and FFT which estimated with an error of 7.14% and 12.2% respectively.

Keywords Oil spill · Cross correlation · Flow measurement

1 Introduction

The use of optical sensors for flow measurements is attractive because of the non-invasiveness of the technique. In particular, optical techniques have proven to be, by far, the most accurate technique for estimating flow rate in the Macondo well spill [1]. However, estimating the velocity field of a turbulent flow from optical data is

A. B. Osman · M. Ovinis (✉) · A. M. M. Mihoob
Mechanical Engineering Department, Universiti Teknologi PETRONAS, 32610 Seri Iskandar, Perak, Malaysia
e-mail: mark_ovinis@utp.edu.my; anotood@yahoo.com

A. O. Mohmmed
Department of Mechanical Engineering, Middle East College, Knowledge Oasis Muscat, Al Rusayl, Muscat, Oman

S. Nisha Basah
School of Mechatronic Engineering, Universiti Malaysia Perlis, 01000 Kangar, Perlis, Malaysia

F. Ahmad et al. (eds.), *ICPER 2020*, Lecture Notes in Mechanical Engineering,
https://doi.org/10.1007/978-981-19-1939-8_1

challenging because of the complex nature of the flow, which includes multi-scale behaviour in both time and space direction. Several optical techniques have been used for estimating the flow rate of oil spill estimation as reviewed in [1, 2], which includes particle image velocimetry (PIV), feature tracking velocimetry (FTV), large eddy velocimetry (LEV), and optical plume velocimetry (OPV). PIV is a common technique usually used for experimental studies and has extensive applications in fluid dynamics. However, PIV failed to estimate accurately the flow rate of the oil spill in case of Macondo well incident [1, 2]. The spatial cross correlation algorithm and the inadequate sizes of interrogation windows usually used in PIV, limited this technique to capture the fast flow of oil spill. Both FTV and LEV techniques, which are based on visible tracking of existing features in the fluid flow space, poorly estimated the flow rate. The bad quality of spill videos led to the inability of these techniques to track visible features such as coherent structures.

The most accurate optical technique used for oil spill flow rate estimation is OPV. This technique was developed by Crone et al. [3], for estimating the flow rate of underwater black smoker, which has similar flow properties to that of the underwater spill. OPV estimates the flow rate based on temporal averaging, in which the turbulent flow variation over time is considered. This could be the main reason behind its better accuracy over other techniques. Moreover, the temporal cross correlation of OPV technique is less sensitive to bias, and requires less computational time [3]. As a comparison, both PIV and OPV use cross correlation algorithm as a step to estimate the flow. However, PIV implements cross correlation spatially, while the OPV is a temporal based on cross correlation, taking only two points in the turbulent flow space. Therefore, PIV is not ideal for capturing turbulent flow due to the variability of the flow over time. This is because of its low temporal resolution (i.e. PIV estimates the velocity from two consecutive images only) and loss of spatial resolution, due to the use of interrogation window for correlation. Therefore, OPV has the advantage of good temporal and spatial resolution as compared to PIV. The proposed technique described in this study comprises the advantages of OPV technique in terms of its temporal and spatial resolution, as well as considering the multi-scale behaviour of the turbulent flow by decomposing into many levels.

The velocity can be estimated by dividing distance over time. To estimate the velocity field using a temporal averaging technique, four steps are required: (i) setting a distance between two points in the flow space, (ii) extracting the signal from these two points (v) cross correlating the two signals, and (iv) detecting the peak correlation coefficients. The time is the time that corresponds to the peak of these coefficients. The most important step for velocity estimation is the cross correlation step. Several algorithms have been used for cross correlation coefficients estimation, and they include, direct cross correlation (DCC), Fast Fourier Transform (FFT) cross correlation, and average square difference function. The DCC algorithm is based on signal amplitude in time domain, while the FFT algorithm is based on frequency information of the signal. However, transforming a signal from time to frequency domain is a trade-off between time information and frequency information.

On the other hand, the wavelet transforms have the ability to decompose a signal/image into many levels and provide both time–frequency information. The

wavelet transforms are applied in several works related to fluid dynamics. These includes investigation of self-similarity and intermittency behaviour in turbulent signals [4, 5], and identification of flow structure [6]. The relation between wavelets and turbulence are discussed by Farge et al. [7]. The application of wavelet transform to turbulent signals are reviewed by Farge [8], as well as using of wavelet for fluid flow simulation [9]. However, in most of these works, the velocity field is already known and wavelet is utilized to understand the turbulent flow behaviour. Fluid motion estimated from image sequences by Dérian et al. [10, 11], combined a differential based algorithm with wavelet expansion. This combination improved the accuracy and the performance of motion estimation algorithm.

In this paper, a new technique based on combining FFT cross correlation and discrete wavelet transform is proposed and named as the DWT-FFT algorithm. The rest of the paper includes material and methods which illustrate the signal simulation model, experimental video data, as well as the developed wavelet-based algorithm, followed by results and discussion and finally the conclusion.

2 Material and Method

2.1 Signal Simulation

A turbulent signal exhibits noisy random behaviour over time [12]. In this work, a random signal is simulated to investigate the accuracy of wavelet based technique. By shifting the simulated signal with known time delay, one can use the DWT-FFT algorithm to estimate the known delay value. The two simulated and shifted signals are generated using Eqs. 1 and 2. The first signal, $S_1(n)$ is a random signal with a length of n, and the second signal $S_2(n)$ is generated by delaying S_1 by a value of d. A random noise $N(n)$ with a certain signal to noise (SNR) is then added to both S_1 and S_2.

$$S_1(n) = s(n) + N(n) \tag{1}$$

$$S_2(n) = s(n-d) + N(n) \tag{2}$$

The magnitude of SNR is calculated as the ratio of signal mean $_{\mu}$, to its standard deviation σ, as shown in Eq. 3:

$$SNR = \frac{\mu}{\sigma} \tag{3}$$

The first signal was delayed using Eq. 1 by a value of d and will be used as ground-truth for evaluating the proposed method. Therefore, the estimation of time delay between the two signals S_1 and S_2 require the following steps:

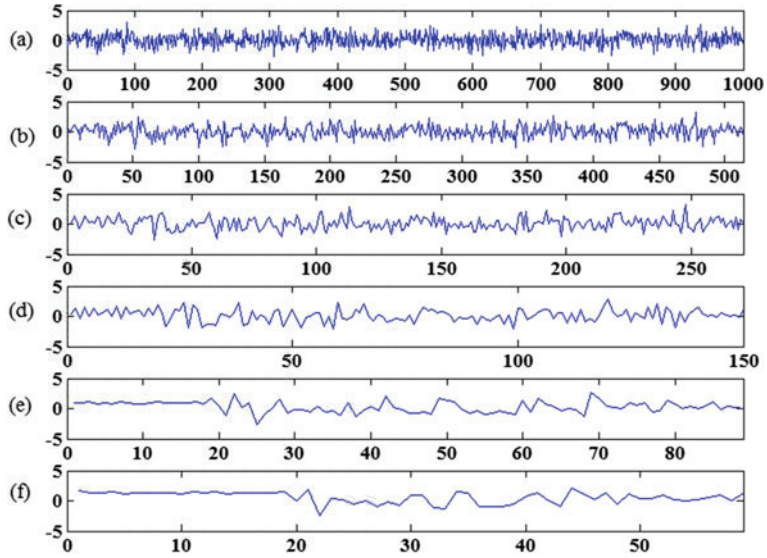

Fig. 1 A sample of the simulated random signal with the reconstructed signals: **a** original signal, **b** level-1, **c** level-2, **d** level-3, **e** level-4 and **f** level-5 signals

- Decompose both signals, S_1 and S_2, into several levels using discrete wavelet transform into approximate and detail information.
- Reconstruct the signal at each level from approximate signal.
- Calculate the time delay between the two signals reconstructed signals for each levels separately using FFT cross correlation algorithm.
- Add noise to the reconstructed signals and estimate the time delay.

In this work, the first signal length is simulated with length of 1000, and delayed by 300 to generate the second signals. Then, the first step to validate our developed algorithm in this paper is to find this delay value. For each level of wavelet, the time delay will be estimated to find out the optimum level of accuracy estimating the delay of random signals. Figure 1 shows a sample of simulated random signals with the reconstructed signals in five levels of wavelet decomposition.

2.2 Turbulent Jet Flow Image Sequence

In order to evaluate the accuracy of the DWT-FFT algorithm, we used an image sequence of a turbulent buoyant jet of Crone et al. [18],who developed an experimental rig to simulate a turbulent buoyant jet in order to develop the OPV technique [3]. The Crone video is available at the website of (http://www.fluidcontinuity.org/research/opv/). Detailed information of this video is summarized in Table1:

Table 1 Video parameters of turbulent buoyant jet

No	Description	Value
1	Video length	30 s
2	Number of frames	994
3	Scale	1 m = 858 pixels
4	Actual flow rate	4.2 pixel/frame
5	Nozzle diameter	18 mm

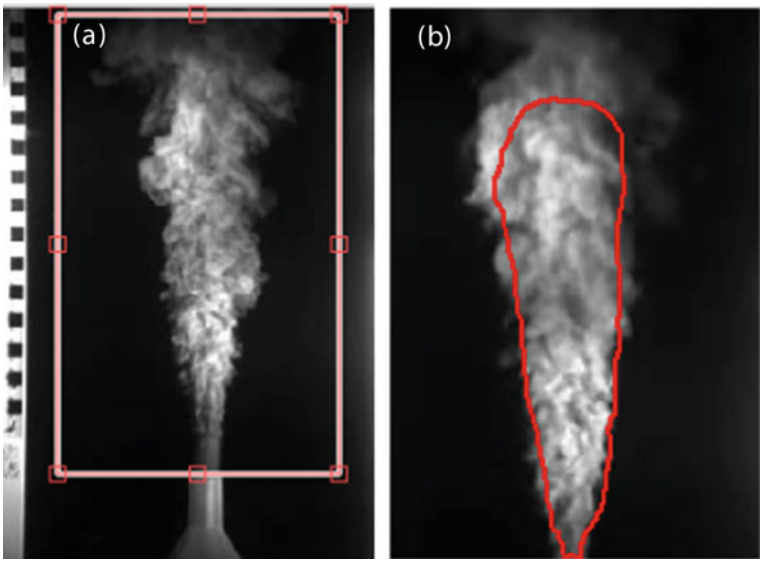

Fig. 2 Sample of turbulent buoyant jet image include **a** original image extracted from Crone video data [3], and **b** cropped image with segmented region

Figure 2, shows a sample of jet flow image which was extracted from the video. The overall video was converted into image sequence, then the flow region is cropped (i.e. rectangular region in Fig. 2(a)) for each image and saved in a 3D matrix in order to estimate its velocity. In order to find the velocity field at the jet flow region, the flow region is segmented as shown by red colour region in Fig. 2b.

2.3 Velocity Field Estimation

The overall methodology for estimating the velocity field from image sequence using the DWT-FFT algorithm is described in Fig. 3.

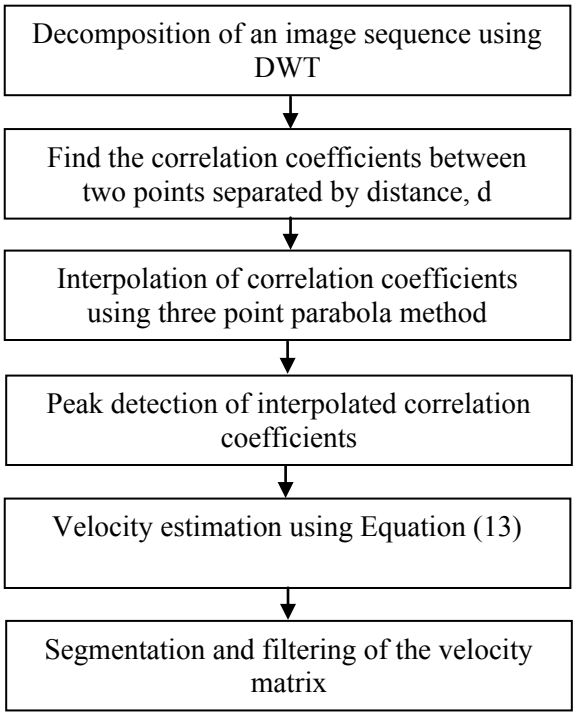

Fig. 3 Steps for estimating the velocity field of jet based on DWT-FFT algorithm

2.4 Discrete Wavelet Transform

The wavelet transform is an extension of the windowed Fourier transform, which has the advantage of presenting any signal in both time–frequency domain. The Fourier transform includes only the frequency information in a small window size. DWT is a common approach in signal/image processing field to decompose any signal/image into multi-levels, in order to analysis the signal/image in both time and frequency domain simultaneously.

If *S(t)* is a time domain signal, the DWT of this signal *D*(*j, k*) can be given by the following equation:

$$D(j,k) = \sum_{t} S(t)\psi_{j,k}(t) \tag{4}$$

where $\psi_{j,k}$(t) is the wavelet coefficient associated with the signal *S(t),* and *j, k* are the wavelet coefficients.

The discrete wavelet phase, $S_P(j, k)$ can be written as:

$$S_p(j,k) = D(j,k)^2 \tag{5}$$

The remaining part of the time series signal in DWT, *r(j,k)* can be given by:

$$r(j,k) = \sum s(t)\phi_{j,k}(t) \tag{6}$$

where $\phi_{j,k}(t)$ denotes the scaling function of the wavelet

$$\phi_{j,k} = 2^{-1/2}\phi_{j,k}(2^{-j}t - k) \tag{7}$$

Then the inverse of DWT can be given by:

$$S(t) = r(j,k)\phi_{j,k}(t) + \sum_{j}\sum_{k} D(i,k)\psi_{j,k}(t) \tag{8}$$

2.5 Correlation Coefficients and Time Delay Estimation

The second step for velocity estimation is the estimation of a time delay between the signals extracted from decomposed image sequence. The delay estimation requires three steps: estimation of correlation coefficients, interpolation, and peak detection of obtained coefficients. To find the correlation coefficients, FFT cross correlation algorithm was applied. First, both signals were transformed in a frequency domain using Fourier transform, then the transformed data multiplied and the inverse found to determine the correlation coefficients. Figure 4 illustrates the steps for finding correlation coefficients using FFT cross correlation algorithm:

Also, the FFT cross correlation algorithm can be formulated by the following Equation:

$$C = ifft(fft(S_1) \cdot conj(fft(S_2)) \tag{9}$$

where C is the correlation coefficients, S_1, S_2 are simulated and delayed signals.

The Fourier Transform of signal S is given by:

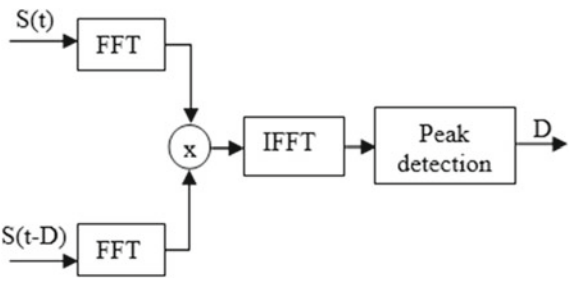

Fig. 4 Correlation coefficients calculation between two signals using FFT-correlation method

$$S_i(k) = \sum_{n=0}^{N-1} S_i(n) \cdot e^{-j\frac{2\pi}{N}n\kappa} \tag{10}$$

and the inverse of FFT is given by using the following equation:

$$S_i(j) = \sum_{k=0}^{N-1} S_i(k) \cdot e^{-j\frac{2\pi}{N}n\kappa} \tag{11}$$

For evaluating the robustness of the DWT-FFT algorithm, two algorithms were selected for comparison purpose – FFT cross correlation algorithm without embedding it in the wavelet domain, and the direct cross correlation (DCC) proposed by Crone et al. [3].

The correlation coefficients $C_{i,j,l}$ can be obtained using DCC algorithm and formulated as:

$$C_{i,j,l} \sum_{k=1}^{N-1} S_{i+d,j,k} \cdot S_{i,j,k+1} \tag{12}$$

where S is the extracted signal, and $_{I,j,l}$ are the number of rows, columns, and a number of images used to estimate the velocity respectively.

Since the correlation coefficients are obtained either by DCC or FFT algorithm, its peak detection will lead to a real time delay value. To find the complete time value with fraction, an interpolation procedure is required. Therefore, a parabola interpolation is applied to the obtained correlation coefficients. Then, the required time delay is the time value that corresponds to the peak of interpolated correlation coefficients. Once the time value is obtained, the velocity u can be easily estimated by the following Equation:

$$u = \frac{d}{\tau} \tag{13}$$

where d is a distance between two points in the turbulent flow space which was taken as 5 pixels as recommended by Crone et al. [3], and τ is the detected time value from the peak of interpolated coefficients. By repeating the same steps for time estimation, the overall velocity field of the jet can be obtained. Finally, due to the presence of noise in the output velocity field matrix, a median filter of size 10 by 10 is applied to smooth the velocity field.

3 Results and Discussion

3.1 Simulation Results

DWT-FFT algorithm is applied to estimate a known time delay between two random signals. A delay value of d = 300 is fixed between the two signals to be used as ground-truth for evaluating this technique. Then, the robustness of the algorithm is evaluated by adding noise to those signals. The range of noise level was measured by the signal-to-noise ratio (SNR) to be between −60 and 60 dB.

For implementing the DWT-FFT algorithm, five levels of wavelet decomposition were found to be enough to obtain reasonably accurate results. Figure 5 shows the relative errors in the estimated time delays for the five wavelet decomposition levels with various level of SNR. Both signal decomposition level and noise level affected directly the accuracy of the algorithm in time delay estimation. More wavelet decomposition level increases the error in time delay estimation. For example, for SNR = −60 dB, the error increased from 0.3% to 22.3% when estimated from level-1 and level-5 signals respectively. Increasing the decomposing signal using DWT usually leads to reduction in the signal length by factor two for each level as shown in Fig. 1. This resulted in uncorrelated signals and inaccurate time value. The second observation is that by increasing the noise level in the signal, the error increases and vice-versa.

To evaluate the stability of the DWT-FFT algorithm against random noise in which the noise power is constant, the time delay value was estimated 10 times for each SNR values and a summary is presented in Table 2. By increasing the SNR, the delay error reduced, as well as a reduction in the variation in delays was observed (i.e. presented by standard deviation).

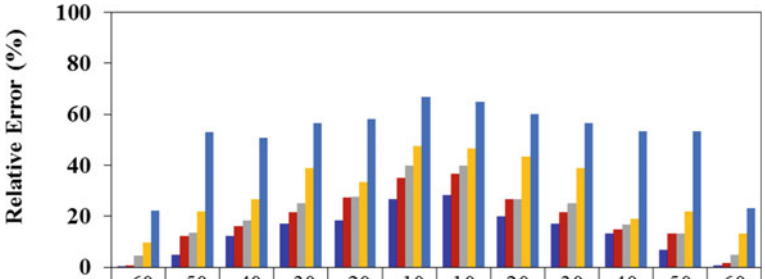

	-60	-50	-40	-30	-20	-10	10	20	30	40	50	60
Level-1	0.3	5	12.3	17	18.3	26.7	28.3	20	17	13.3	6.7	0.7
Level-2	0.7	12.3	16	21.7	27.3	35	36.7	26.7	21.7	15	13.3	1.7
Level-3	4.7	13.7	18.3	25	27.7	40	40	26.7	25	16.7	13.3	5
Level-4	9.7	22	26.7	39	33.3	47.7	46.7	43.3	39	19	22	13.3
Level-5	22.3	53	50.7	56.7	58.3	66.7	65	60	56.7	53.3	53.3	23.3

Fig. 5 Errors in estimated time delay for 5 wavelet decomposition with various SNR level

Table 2 Estimated time delay (Average, standard deviation, and error) for 10 runs in each case of SNR

Error (%)	RMSE (%)	Standard Deviation	Average of delay	SNR
59.1	10.08	31.89	122.61	5
39.7	7.27	22.99	180.82	10
28.4	8.99	28.43	21.86	20
26.7	6.27	19.84	219.97	30
23	3.4	10.75	231.07	40
19.9	5.31	16.79	240.31	50
16.9	5.7	18.01	249.23	60

3.2 Turbulent Jet Flow Results

The DWT-FFT algorithm is evaluated with real experimental image sequence of turbulent jet flow. These image sequences were extracted from Crone's video. The velocity field for each wavelet levels was estimated using the DWT-FFT algorithm. Figure 6 shows the estimated jet velocity field for four wavelet decomposition levels. The obtained velocity field was scaled from zero to the magnitude of the actual velocity i.e. 4.2 pixel/frame (refer to Table.1). Only the jet flow region is presented and its background filled by white colour.

Therefore, by increasing the wavelet decomposition, noisy velocity field was obtained. The artifact errors therefore increased (see Fig. 6c and d). This is due to the loss of energy from one level to the next during wavelet decomposition and reconstruction procedures. Increasing the number of decomposition levels usually increase the error in signal reconstruction. A good representation of the flow field can be obtained by first and second levels of decomposition as shown in Fig. 6a and b. The obtained velocity field in these two levels is similar to what is expected from jet theory, in which the maximum velocity should be at pure jet region near to the nozzle, while the velocity starts decaying in stream-wise direction. A smooth velocity field was observed at the fully developed region far from the nozzle area in the estimation from level-2 and level-3 (i.e. Figure 6b, c), while noise velocity field was obtained from level-3 and level-4.

The accuracy of DWT-FFT algorithm was based on proper selection of wavelet function that can be used for decomposing the turbulent signals. Four wavelet functions namely Daubechies, Symlet, Coiflet and Haar wavelets were selected for comparison purpose. Figure 7 shows the velocity field obtained by applying these different wavelets at level-2.

Almost similar velocity field was obtained using the four wavelets with small difference. Although there was some similarities, the quantification of nozzle velocity showed some variation by the use of those wavelets.

Figure 8 shows the error in nozzle velocity estimation using the different wavelets for three level of decomposition. The best result was obtained by Coiflet wavelet in

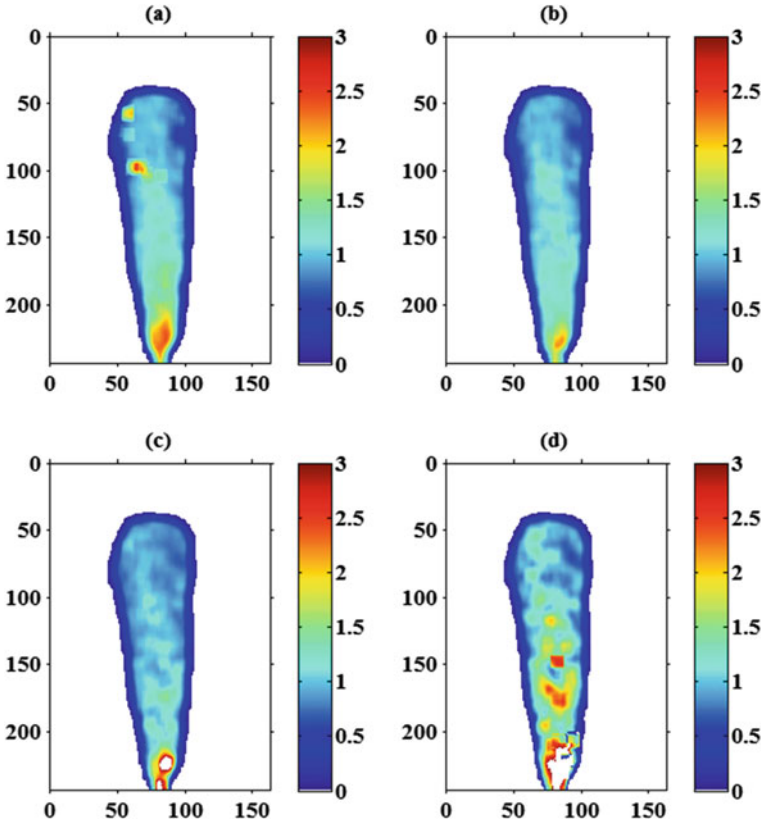

Fig. 6 Velocity field for three levels of wavelet decomposition using Daubechies wavelet function at: **a** Level-1 **b** Level-2 **c** Level-3 and **d** Level-4

the first level of decomposition with an error of 0.7%. Higher errors were obtained when the nozzle velocity was estimated from level-2 and level-3.

One of the important factors that affect the accuracy of DWT-FFT technique is the vanishing moment of wavelet function used. To investigate the effect of vanishing moment in the nozzle velocity estimation, the Coiflet wavelet with standard vanishing moment ranged from 1 to 5 was applied. Figure 9 illustrates the relative error estimated in nozzle velocity estimation as a relation to the vanishing moment. By increasing the vanishing moment from 1 to 5, the error reduced by a percentage of 73%. The same conclusion obtained by Dérian et al. [11] when Daubechies wavelet was used with different vanishing moment for motion estimation. Therefore, the best vanishing moment when Coiflet function was used in nozzle velocity estimation is equal to 5.

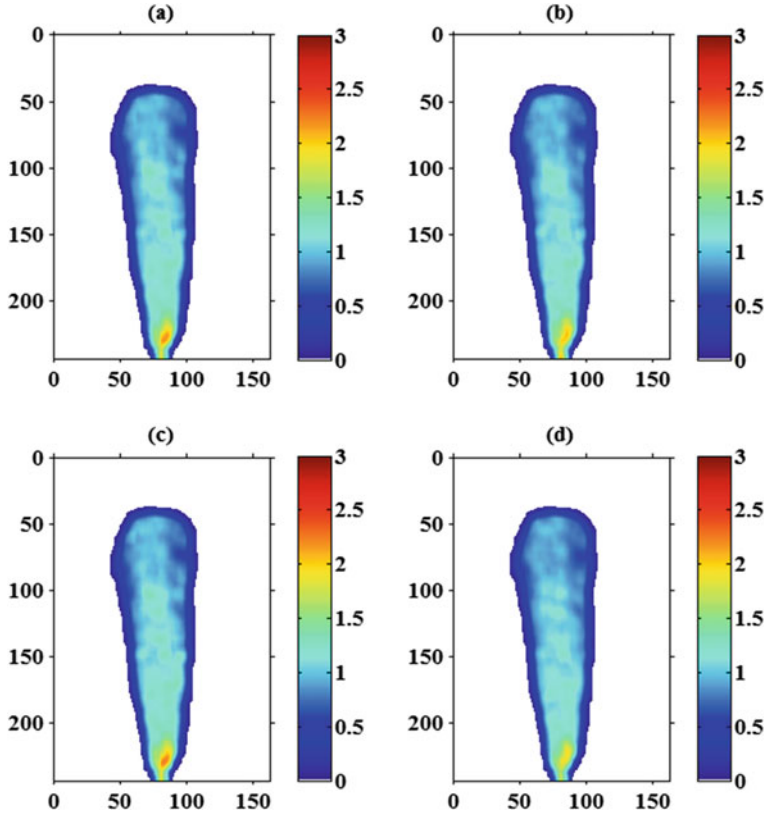

Fig. 7 Jet velocity field obtained using different wavelet functions: **a** Daubechies, **b** Symlet, **c** Coiflet and **d** Haar wavelet

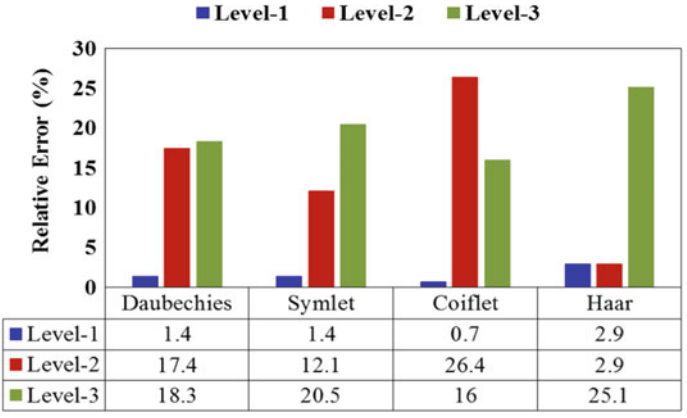

	Daubechies	Symlet	Coiflet	Haar
Level-1	1.4	1.4	0.7	2.9
Level-2	17.4	12.1	26.4	2.9
Level-3	18.3	20.5	16	25.1

Fig. 8 Relative errors in nozzle velocity estimation using different wavelet functions at various decomposition levels

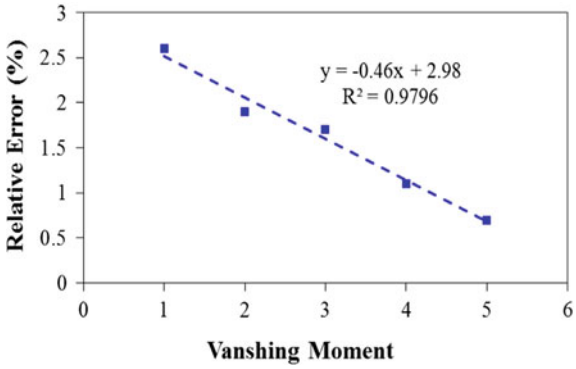

Fig. 9 The vanishing moment effect in nozzle velocity estimation

Table 3 Comparison between various algorithms

No	Algorithm	Estimated velocity	Relative error (%)
1	DCC	3.90	7.14
2	FFT-correlation	3.69	12.2
3	DWT-FFT	4.17	0.7

3.3 Comparison to Classical Algorithms

Since the main objective of this work is to develop an alternative technique for accurately estimating the nozzle velocity, the best result obtained using the developed DWT-FFT algorithm is based on using Coiflet wavelet with vanishing moment of 5 and by estimating the velocity field from the reconstructed signals of the first level of wavelet decomposition.

The accuracy of DWT-FFT algorithm was compared to two other classical algorithms namely DCC and FFT algorithms. Both algorithms were applied to estimate the velocity field of the jet flow and the nozzle velocity. Table 3 shows a comparison between the results obtained by using the three algorithms. The actual nozzle velocity, 4.2 pixel/frame, obtained by Crone et al. [3] was used as the ground truth for validation. The accuracy DWT-FFT algorithm is better than the accuracy of DCC and FFT algorithm.

4 Conclusion

In this paper, a new technique was proposed for turbulent flow estimation from image sequence. The proposed technique is based on wavelet transform, which is named as DWT-FFT. Various parameters were investigated to test the accuracy of the DWT-FFT including wavelet decomposition level, wavelet function, and the vanishing moment of wavelet function. The DWT-FFT algorithm was validated using both simulated

signals and image sequence. Both simulated and experimental results showed that the DWT-FFT algorithm was more sensitive to the wavelet decomposition level and the signal noise. Increasing the decomposing level increased the error in time delay estimation. Also increasing the wavelet decomposition levels resulted in a noisy velocity field. The optimum condition for the developed algorithm was achieved using Coiflet wavelet with a vanishing moment of 5. The DWT-FFT algorithm was the most robust of the algorithms and estimated the nozzle velocity with an error of 0.7%. For future work, experimental work will be conducted by building a rig to simulate a turbulent jet flow. Then, the DWT-FFT algorithm will be applied to estimate the velocity field, and more investigation will be conducted on the effect of changing nozzle flow rate on the accuracy of the algorithm.

Acknowledgements The authors would like to express their appreciation to Universiti Teknologi PETRONAS for supporting this work under YUTP 015LC0-180.

References

1. McNutt MK, Camilli R, Crone TJ, Guthrie GD, Hsieh PA, Ryerson TB et al (2012) Review of flow rate estimates of the Deepwater Horizon oil spill. Proc Natl Acad Sci 109:20260–20267
2. Lehr B, Aliseda A, Bommer P, Espina P, Flores O, Lasheras J et al (2010) Deepwater horizon release estimate of rate by PIV. Report to the US Dept of interior
3. Crone TJ, McDuff RE, Wilcock WS (2008) Optical plume velocimetry: a new flow measurement technique for use in seafloor hydrothermal systems. Exp Fluids 45:899–915
4. Xu G, Wan B, Zhang W (2006) Application of wavelet multiresolution analysis to the study of self-similarity and intermittency of plasma turbulence. Rev Sci Instrum 77:083505
5. Ruppert-Felsot J, Farge M, Petitjeans P (2009) Wavelet tools to study intermittency: application to vortex bursting. J Fluid Mech 636:427–453
6. Hui L (1998) Flow structure identification of a turbulent shear flow with use of wavelet statistics
7. Farge M, Kevlahan N, Perrier V, Goirand E (1996) Wavelets and turbulence. Proc IEEE 84:639–669
8. Farge M (1992) Wavelet transforms and their applications to turbulence. Annu Rev Fluid Mech 24:395–458
9. Kim T, Thürey N, James D, Gross M (2008) Wavelet turbulence for fluid simulation. ACM Trans Graph (TOG) 50
10. Dérian P, Héas P, Herzet C, Mémin É (2012) "Wavelet-based fluid motion estimation. Scale space and variational methods in computer vision. Springer, pp 737–748
11. Dérian P (2012) Wavelets and fluid motion estimation. Université Rennes 1, 2012
12. Ferré-Giné J, Rallo R, Arenas A, Giralt F (1997) Extraction of structures from turbulent signals. Artif Intell Eng 11:413–419

Influence of Swirl Flow Pattern in Single Tube Burner on Turbulent Flame Blow-Off Limit

Hasanain A. Abdul wahhab

Abstract Blow-off limits for a premixed turbulent flame are influenced by swirl flow pattern. The objective of the current paper is to present experimental investigations and numerical simulation for identifying and evaluating the influence of changing the swirl intensity by increasing the mixture flow rate on the blow-off limits at different equivalence ratio values (LPG-air mixtures). Both, experimental and numerical observations for swirling turbulent flames at different conditions close to blow-off and after blow-off were discussed. The numerical analysis was carried out using ANSYS 17.0 FLUENT Premixed Model, also called Turbulent Flame Speed Closure (TFSC) model. By varying the flow rate of the mixture, the blow-off velocity in lean and rich mixing sides was determined. It has been realized that when the mixture of unburned gases flow approaches to the combustion zone, a sudden expansion of the flow field occurs; also, the inner and outer flow diverges due to the swirl momentum. Also, the mean axial velocity decreases with the increase of expansion distance, as it depends on the conservation of mass law. The results elucidated that increasing swirl intensity of unburned gas increases the flame separation distance, also the blow-off limit in the lean fuel side needs relatively to fewer values from the velocities compared to the rich fuel side.

1 Introduction

In the past few years, improving premixed combustion operations in gas turbine and aircraft engines have become a significant challenge in order to reduce NOx emissions providing a high mixing quality and low flame temperature. Moreover, the design of modern high performance propulsion systems suffers from major problem of combustion instability [1, 2]. Combustion instability generates an important issue concerning with self sustained combustion oscillations in the combustion chamber, as the pressure fluctuations with unstable rise in temperature are the cause of this closed loop coupling. More so, all these problem can induce unstable operations

H. A. Abdul wahhab (✉)
Department of Mechanical Engineering, University of Technology-Iraq, Baghdad, Iraq
e-mail: 20085@uotechnology.edu.iq

F. Ahmad et al. (eds.), *ICPER 2020*, Lecture Notes in Mechanical Engineering,
https://doi.org/10.1007/978-981-19-1939-8_2

caused to increased heat transfer at combustion chamber walls, finally may lead to total blow off [3, 4]. Also, many studies tested all the ways to determine the low typical frequency oscillations which cause large mechanical vibrations in the combustion system that may ultimately result in blow off [5–7]. The use of swirl combustors in gas turbine combustion systems is one of the best improvements to its ability to stabilize flame within wide ranges of equivalence ratios [8, 9]. Therefore, the design and development of combustion systems in gas turbines are required entirely to encounter numerous basic design elements, like a high efficiency of combustion that covers broad working limits, low greenhouse gas emissions, and low limits of flame stability [10–12]. Shanbhogue et al. [13] demonstrated that lean-premixed turbulent flames are more susceptible to blow-off. Also, they confirmed that blow-off limit of lean turbulent flames uaually starts by generation of local swirls along the combustor region where the local momentum rate exceeds the critical limit. Steinberg et al. [14] analyzed the shape of flame front for different phases in a combustor region; it is an important feature that controls the uniformity of the temperature in the burnt gases at the combustor outlet. Chan et al. [2] studied the weak swirl to investigate in stabilize propagating open premixed turbulent flames, for a range of the swirl numbers between 0.05 and 0.3, their experiments used a jet burner. They noted that the measured tangential component for flame velocity within the turbulent zone (at downstream of the burner edge) was close to zero for the entire radius of the burner, which they concluded that the flame itself was unaffected by the swirl. Rajasegar et al. [7] tested new geometrical adaptations to generic high swirl-center-fan burner to change the swirl number in order to study blow-off limit. They explained that the critical value of swirl number required for the occurrence of blow-off, depended on: Reynolds number for fuel–air flow, equivalence ratio, and swirl design features. Varying the total reactants flows from 400 to 1650 SLPM showed that increased blow-off flame behaviour. This effect was attributed to the influence of the sudden pressure drop between unburned and burned gases across the flame front which increases with total flow. Zhang et al. [15] prepared blow-off experiments of turbulent flame using $CH_4/H_2/CO$ blends on a high-pressure, high-vortex burner designed to match gas turbine conditions. Their results appeared that hydrogen controls the lean blow-off limits, and many other physically meaningful variables (laminar burning velocity, turbulent flame speed, thermal diffusivity) are simply functions of percentage of hydrogen. Generally, many techniques have been used to develop traditional deigns of burner for ensuring gas turbines steady working. These methods are either the development of aerodynamics and then turbulence in the swirling flow field in the chamber of combustion to expand stability, or using the substituted fuels for reducing the combustion impact upon the surroundings [16–18]. On the other hand, there is little information on the impact of swirl patterns for turbulent flames on the limits near blow-off [19]. Therefore, interest in observing the mechanism of the flame blow-off has increased because of the need to operate disturbed flame incinerators under different conditions: for different fuels, the application of available swirling techniques, close to the blow-off limits [20–22]. There is a limited research available upon the swirling spray flames behaviour throughout the blow-off; Dawson et al. [23] studied the cases of spray flames for premixed and non-premixed combustion in the